

Supporting Information for

**Terminal alkyl substitution in A-D-A-type nonfullerene acceptor:  
Simultaneous improvement in open-circuit voltage and short-circuit current  
for efficient indoor power generation**

*Hwa Sook Ryu,<sup>a</sup>† Hyun Gyeong Lee,<sup>b</sup>† Sang-Chul Shin,<sup>c</sup>† Jooho Park,<sup>a</sup> Sang Hyeon Kim,<sup>d</sup> Eun Ji Kim,<sup>b</sup> Tae Joo Shin,<sup>e</sup> Jae Won Shim, \*<sup>d</sup> Bumjoon J. Kim, \*<sup>b</sup> and Han Young Woo \*<sup>a</sup>*

<sup>a</sup>Department of Chemistry, Korea University, Seoul, 02841, Republic of Korea.

<sup>b</sup>Department of Chemical and Biomolecular Engineering, Korea Advanced Institute of Science and Technology (KAIST), Daejeon, 34141, Republic of Korea.

<sup>c</sup>Division of Electronics and Electrical Engineering, Dongguk University, Seoul, 04620, Republic of Korea.

<sup>d</sup>School of electrical engineering, Korea university, Seoul, 02841, Republic of Korea.

<sup>e</sup>UNIST Central Research Facilities, Ulsan National Institute of Science and Technology (UNIST), Ulsan, 44919, Republic of Korea.

E-mail: hywoo@korea.ac.kr, bumjoonkim@kaist.ac.kr, jwshim19@korea.ac.kr

**Characterization:**  $^1\text{H}$  and  $^{13}\text{C}$  NMR spectra were recorded using a Bruker Advance III HD system operating at 500 and 125 MHz, respectively. UV-vis spectra were obtained using a JASCO V-630 spectrophotometer. CV data were measured using a Versa STAT3 (Princeton Applied Research) with a three-electrode cell in 0.1 M of tetrabutylammonium tetrafluoroborate ( $\text{Bu}_4\text{NBF}_4$ ) in  $\text{CH}_3\text{CN}$  at a scan rate of 50 mV s $^{-1}$  (employing a platinum wire as a counter electrode, platinum electrode coated with a semiconductor film as a working electrode, and  $\text{Ag}/\text{Ag}^+$  electrode as a reference electrode). TGA (TGA n-1000) and DSC (DSC 4000) were conducted at a heating and cooling rate of 10 °C min $^{-1}$  under  $\text{N}_2$ . 2D GIWAXS was conducted at the 9A (U-SAXS) at the Pohang Accelerator Laboratory, Pohang, Republic of Korea. The surface morphology of the films was characterized using AFM (Park NX 10) in the tapping mode, whereas the thickness was measured using AFM (advanced scanning probe microscope, XE-100, PSIA). Morphologies were also examined using transmission electron microscopy (TEM, Tecnai F30 ST) at 300 kV.

**Table S1.** Summary of indoor photovoltaic characteristics under halogen lamp.

Donor:Acceptor	Light source	$V_{\text{OC}}$ [mV]	$J_{\text{SC}}$ $\mu\text{A cm}^{-2}$	FF [%]	PCE [%]	$P_{\text{out}}$ $\mu\text{W cm}^{-2}$
P3HT:ICBA <sup>[1]</sup>	halogen (1000-lx)	700	74.7	68.2	0.4	35.7
PDTBTBz- 2F <sub>anti</sub> :PC <sub>71</sub> BM <sup>[2]</sup>	halogen (1000-lx)	809	116.8	70.2	0.8	66.3
P3HT:PC <sub>71</sub> BM <sup>[2]</sup>	halogen (1000-lx)	486	71.8	71.0	0.3	24.8
PBDB-T:PC <sub>71</sub> BM <sup>[2]</sup>	halogen (1000-lx)	669	108.3	71.0	0.6	51.4
PTB7:PC <sub>71</sub> BM <sup>[2]</sup>	halogen (1000-lx)	576	171.4	67.4	0.8	66.5
P3HT:ICBA <sup>[3]</sup>	halogen (500-lx)	647	45.9	57.0	0.3	16.9
P3HT:ICBA <sup>[4]</sup>	halogen (1000-lx)	717	79.6	73.2	0.5	41.8

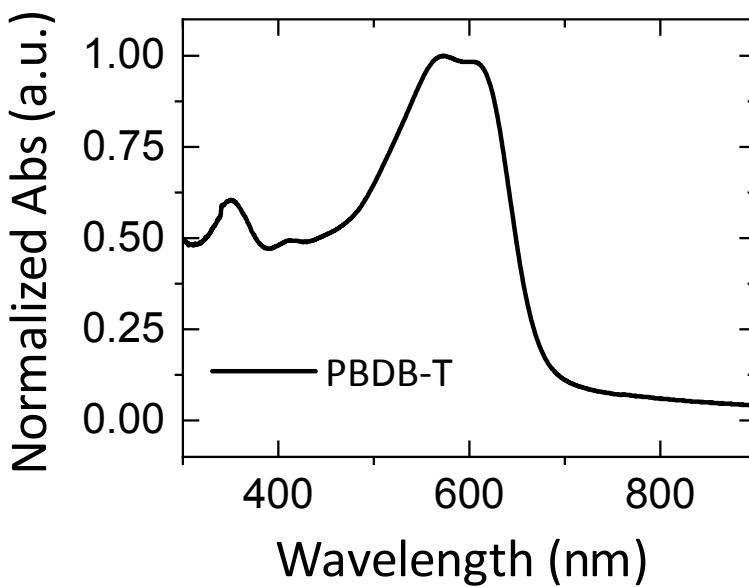


**Figure S1.** Normalized UV-vis absorption spectrum of PBDB-T in film.

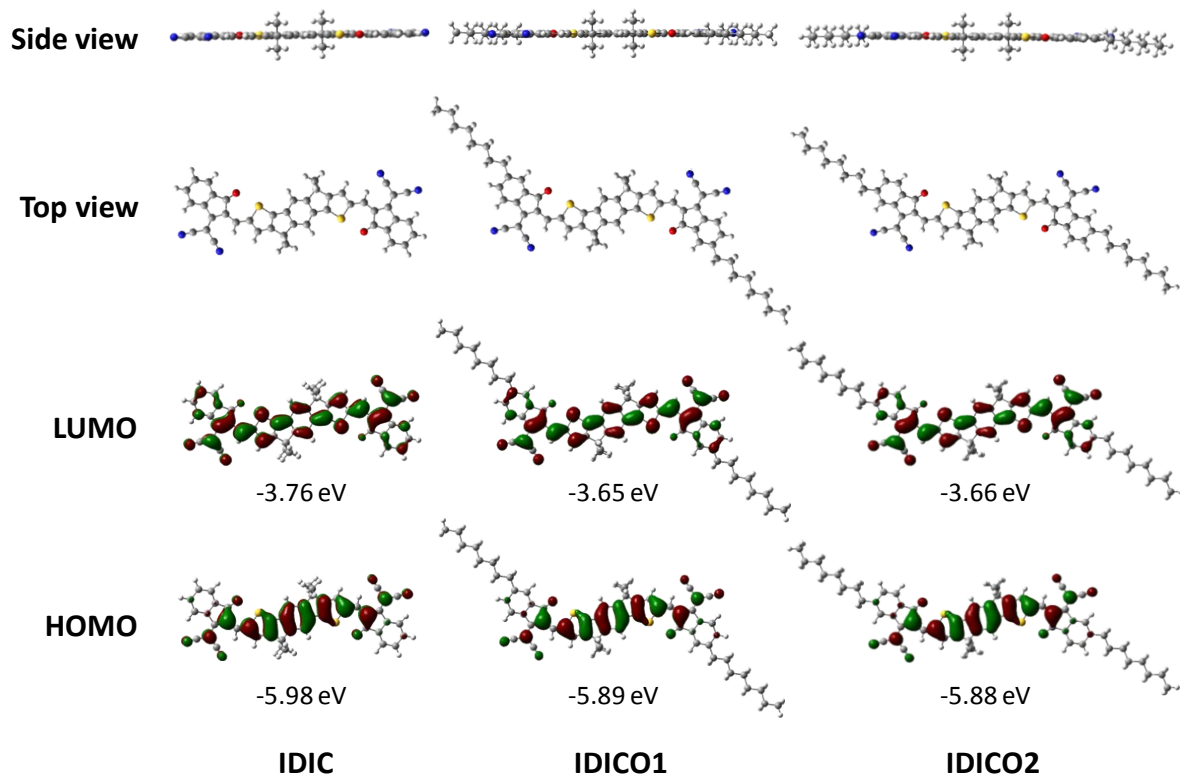


**Figure S2.** Energy-minimized structures, FMO structures of IDIC, IDICO1, and IDICO2 by DFT at the B3LYP/6-31G (d,p) level (C: gray, N: blue, O: red, S: yellow).

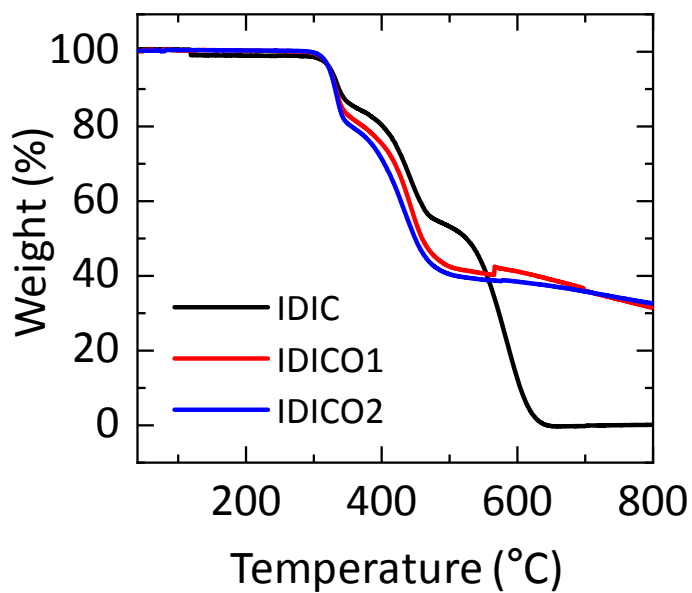


**Figure S3.** TGA thermograms of IDIC, IDICO1, and IDICO2.

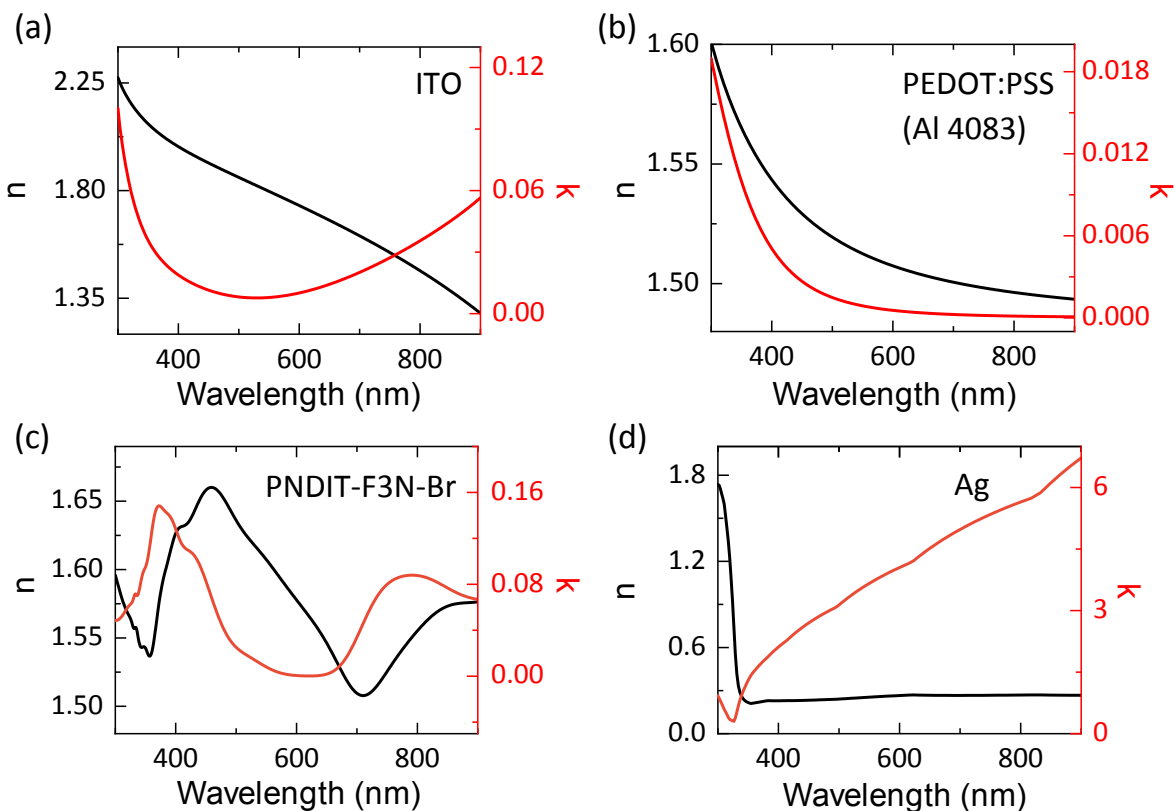


**Figure S4.** Complex refractive index ( $n$  and  $k$ ) spectra of (a) ITO, (b) PEDOT:PSS (Al 4083), (c) PNDIT-F3N-Br and (d) Ag of tested photovoltaic devices.

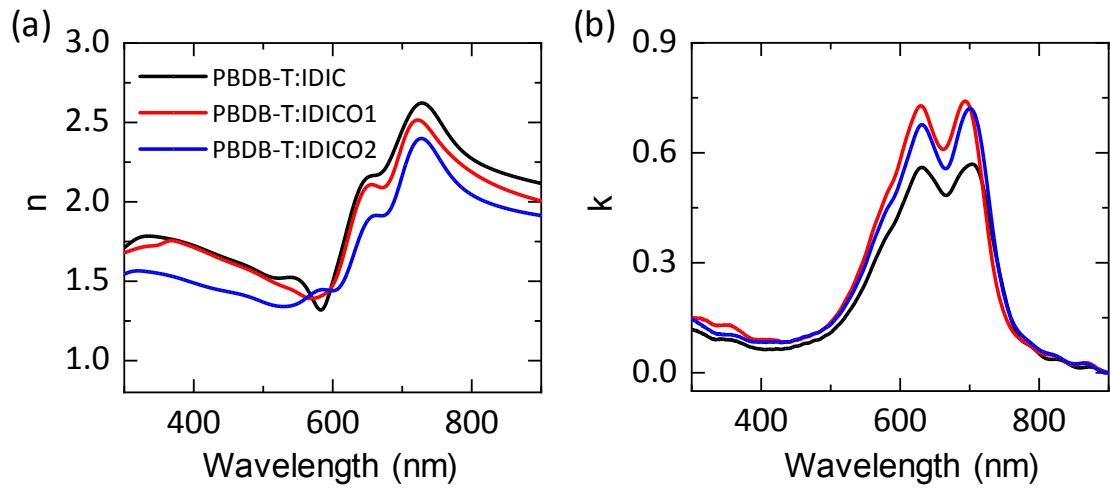


**Figure S5.** (a)  $n$  and (b)  $k$  Spectra of PBDB-T:IDIC, PBDB-T:IDICO1 and PBDB-T:IDICO2 blend films.

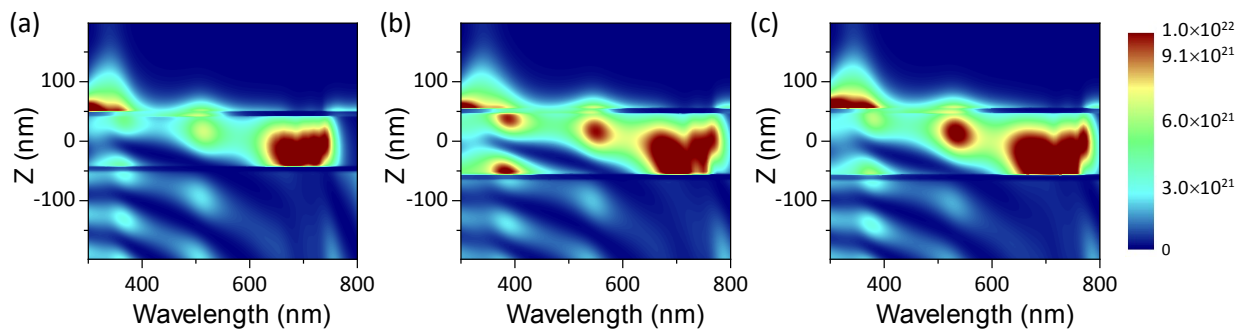


**Figure S6.** Absorption profiles of (a) PBDB-T:IDIC, (b) PBDB-T:IDICO1 and (c) PBDB-T:IDICO2 by FDTD simulation.

**Table S2.** Photovoltaic parameters of PBDB-T:IDIC, PBDB-T:IDICO1, and PBDB-T:IDICO2 with varying LED intensity (200-lx to 2000-lx).

Acceptor	$V_{OC}$ [V]	$J_{SC}$ [ $\mu\text{A cm}^{-2}$ ]	FF	PCE [%]	Max. Power Density [ $\mu\text{W cm}^{-2}$ ]
200-lx (Irradiance, $P_{in} = 0.08 \text{ mW cm}^{-2}$ )					
IDIC	0.59	22.5	0.47	7.80	6.2
IDICO1	0.65	37.5	0.46	14.02	11.2
IDICO2	0.67	41.2	0.43	14.84	11.9
500-lx (Irradiance, $P_{in} = 0.17 \text{ mW cm}^{-2}$ )					
IDIC	0.63	45.0	0.54	9.01	15.3
IDICO1	0.70	72.5	0.53	15.82	26.9
IDICO2	0.71	79.2	0.47	15.55	26.4
800-lx (Irradiance, $P_{in} = 0.21 \text{ mW cm}^{-2}$ )					
IDIC	0.65	67.4	0.58	12.10	25.4
IDICO1	0.72	105.8	0.57	20.68	43.4
IDICO2	0.73	113.0	0.50	19.64	41.2
1000-lx (Irradiance, $P_{in} = 0.28 \text{ mW cm}^{-2}$ )					
IDIC	0.67	73.6	0.57	11.71	32.8
IDICO1	0.76	120.7	0.61	20.41	57.2
IDICO2	0.74	112.7	0.59	19.16	53.7
1500-lx (Irradiance, $P_{in} = 0.42 \text{ mW cm}^{-2}$ )					

IDIC	0.68	115.3	0.62	11.57	48.6
IDICO1	0.75	176.1	0.61	19.18	80.6
IDICO2	0.76	180.5	0.55	17.96	75.4
2000-lx (Irradiance, $P_{in} = 0.58 \text{ mW cm}^{-2}$ )					
IDIC	0.69	154.2	0.63	11.56	67.0
IDICO1	0.76	233.0	0.62	18.93	109.8
IDICO2	0.77	233.4	0.58	17.97	104.2

**Table S3.** Photovoltaic parameters of PBDB-T:IDIC, PBDB-T:IDICO1, and PBDB-T:IDICO2 with varying the halogen lamp intensity (200-lx to 2000-lx).

Acceptor	$V_{OC}$ [V]	$J_{SC}$ [ $\mu\text{A cm}^{-2}$ ]	FF	PCE [%]	Max. Power Density [ $\mu\text{W cm}^{-2}$ ]
200-lx (Irradiance, $P_{in} = 3.1 \text{ mW cm}^{-2}$ )					
IDIC	0.66	68.5	0.59	0.86	26.7
IDICO1	0.70	78.0	0.54	0.95	29.5
IDICO2	0.72	98.4	0.49	1.17	34.7
500-lx (Irradiance, $P_{in} = 5.4 \text{ mW cm}^{-2}$ )					
IDIC	0.69	133.3	0.64	1.09	58.9
IDICO1	0.74	154.9	0.62	1.32	71.1
IDICO2	0.76	182.9	0.56	1.44	77.8
800-lx (Irradiance, $P_{in} = 7.5 \text{ mW cm}^{-2}$ )					
IDIC	0.71	198.8	0.66	1.24	93.2

IDICO1	0.76	228.1	0.63	1.46	109.2
IDICO2	0.78	256.3	0.59	1.57	117.9
1000-lx (Irradiance, $P_{in} = 8.4 \text{ mW cm}^{-2}$ )					
IDIC	0.71	202.7	0.65	1.12	102.1
IDICO1	0.77	252.4	0.66	1.53	132.4
IDICO2	0.77	271.2	0.63	1.56	141.4
1500-lx (Irradiance, $P_{in} = 10.6 \text{ mW cm}^{-2}$ )					
IDIC	0.73	315.0	0.69	1.50	158.7
IDICO1	0.78	377.2	0.65	1.80	191.2
IDICO2	0.80	401.0	0.64	1.94	205.3
2000-lx (Irradiance, $P_{in} = 13.4 \text{ mW cm}^{-2}$ )					
IDIC	0.74	391.3	0.69	1.49	199.8
IDICO1	0.80	485.8	0.66	1.91	256.5
IDICO2	0.81	506.3	0.64	1.96	262.5

**Table S4.** Summary of SCLC charge mobilities.

	$\mu_h [\text{cm}^2\text{V}^{-1}\text{s}^{-1}]$	$\mu_e [\text{cm}^2\text{V}^{-1}\text{s}^{-1}]$	$\mu_h/\mu_e$
IDIC	-	$1.87 \times 10^{-5}$	-
IDICO1	-	$4.05 \times 10^{-5}$	-
IDICO2	-	$4.76 \times 10^{-5}$	-
IDIC:PBDB-T	$2.27 \times 10^{-4}$	$3.52 \times 10^{-5}$	6.45
IDICO1:PBDB-T	$2.02 \times 10^{-4}$	$4.50 \times 10^{-5}$	4.49
IDICO2:PBDB-T	$1.28 \times 10^{-4}$	$2.37 \times 10^{-5}$	5.40

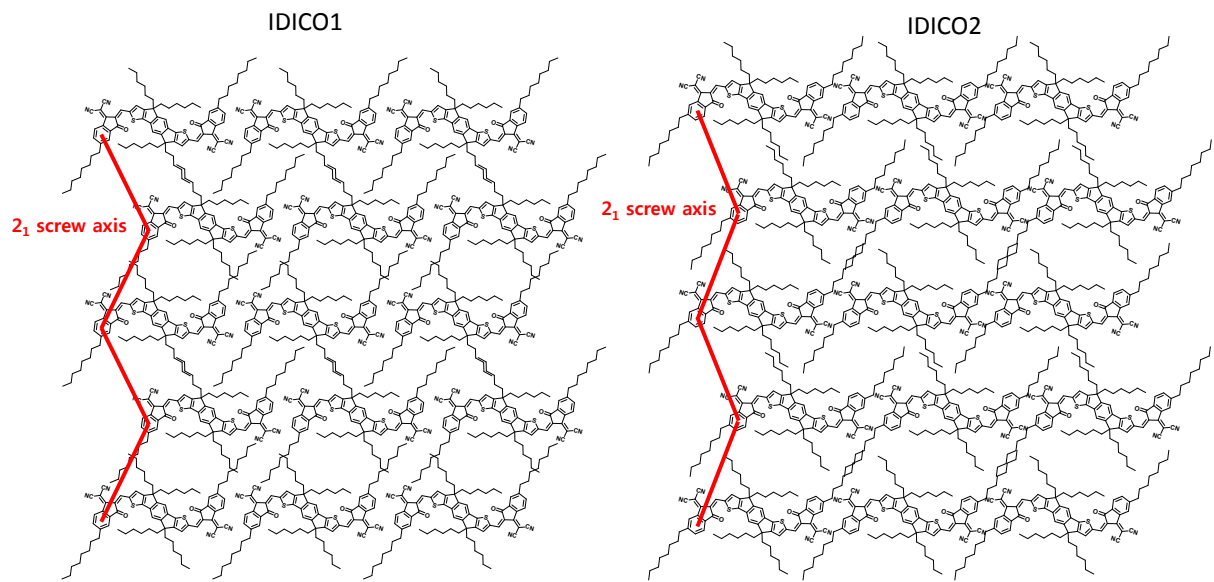


**Figure S7.** Packing structures estimated from GIWAXS data for pristine IDICO1 and IDICO2 films.

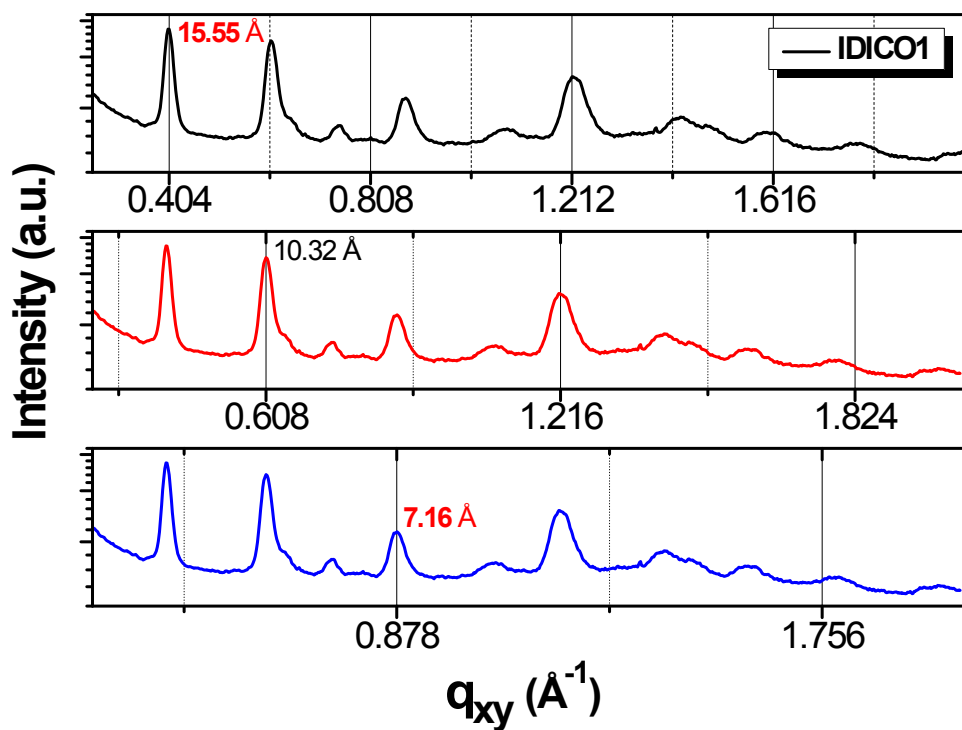


**Figure S8.** In-plane 1D GIWAXS profiles of IDICO1 film.

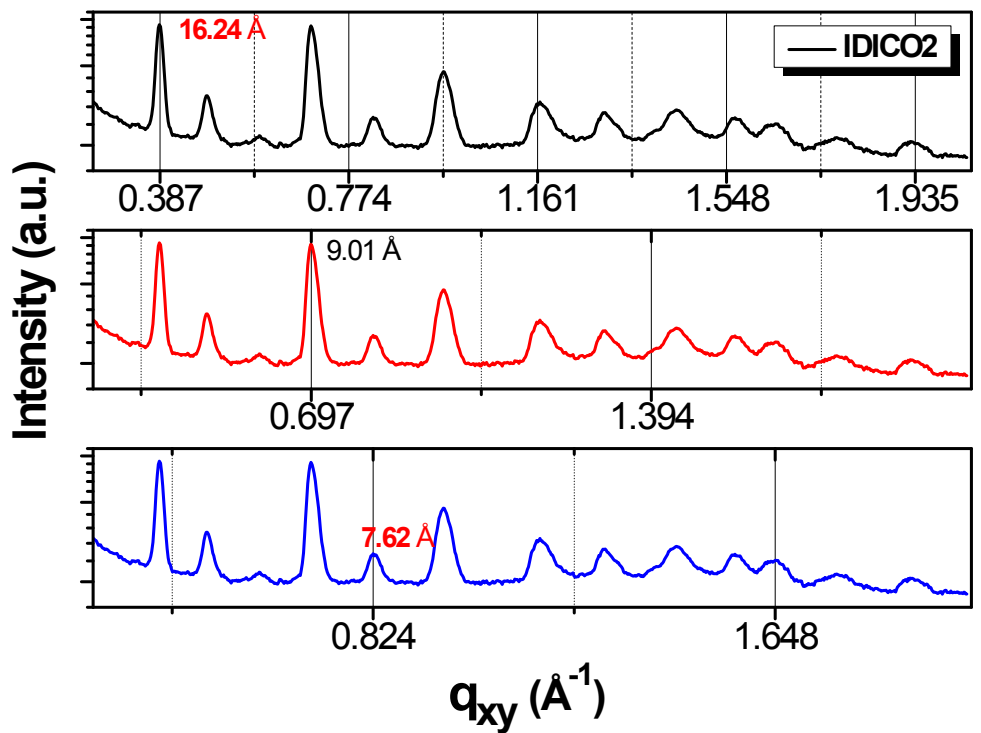


**Figure S9.** In-plane 1D GIWAXS profiles of IDICO2 film.

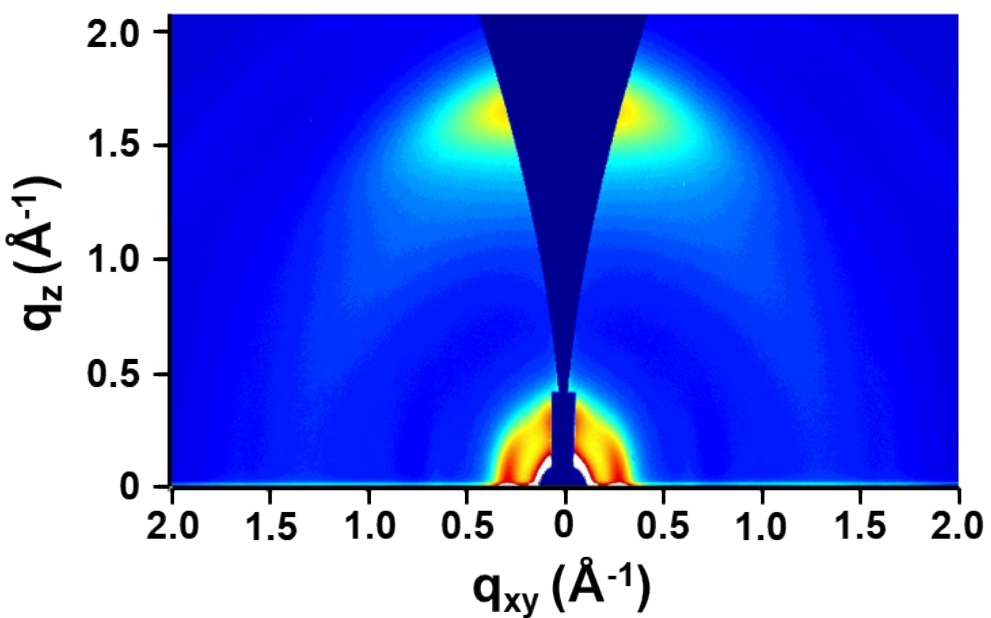


**Figure S10.** 2D GIWAXS image of PBDB-T film.

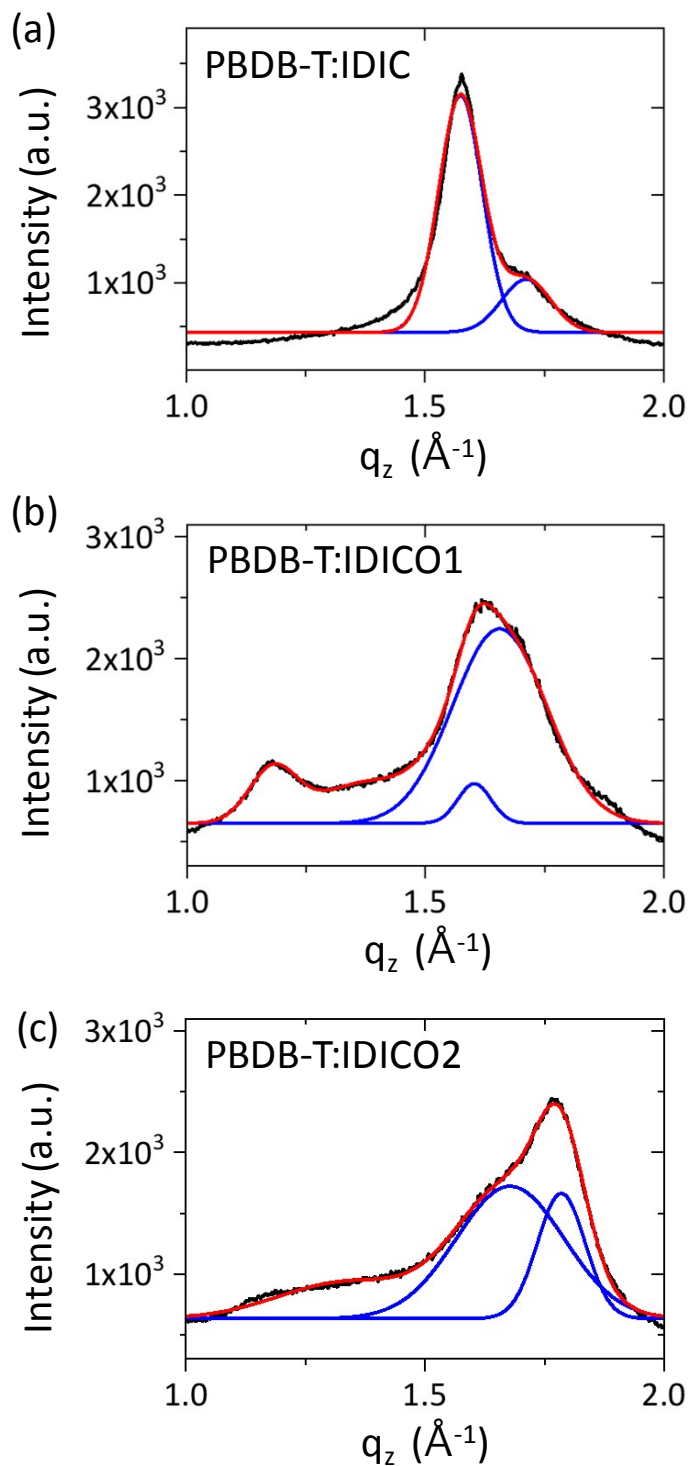


**Figure S11.** Multiple-peak Gaussian fitting of the OOP (010) peak for (a) PBDB-T:IDIC, (b) PBDB-T:IDICO1 and (c) PBDB-T:IDICO2.

**Table S5.** Summary of GIWAX packing parameters.

		q [Å <sup>-1</sup> ]	d-spacing
PBDB-T	(100) <sup>a)</sup>	0.27	22.99
	(010) <sup>b)</sup>	1.62	3.88
IDIC:PBDB-T	(100) <sup>a)</sup>	0.28	22.34
	(010) <sup>b)</sup>	1.57	3.99
	(010) <sup>b)</sup>	1.71	3.67
IDICO1:PBDB-T	(100) <sup>a)</sup>	0.29	21.64
	(010) <sup>b)</sup>	1.60	3.92
	(010) <sup>b)</sup>	1.66	3.80
IDICO2:PBDB-T	(100) <sup>a)</sup>	0.31	20.37
	(010) <sup>b)</sup>	1.68	3.74
	(010) <sup>b)</sup>	1.79	3.52

<sup>a)</sup> (100) peak along the q<sub>xy</sub> direction; <sup>b)</sup> (010) peak in the q<sub>z</sub> direction

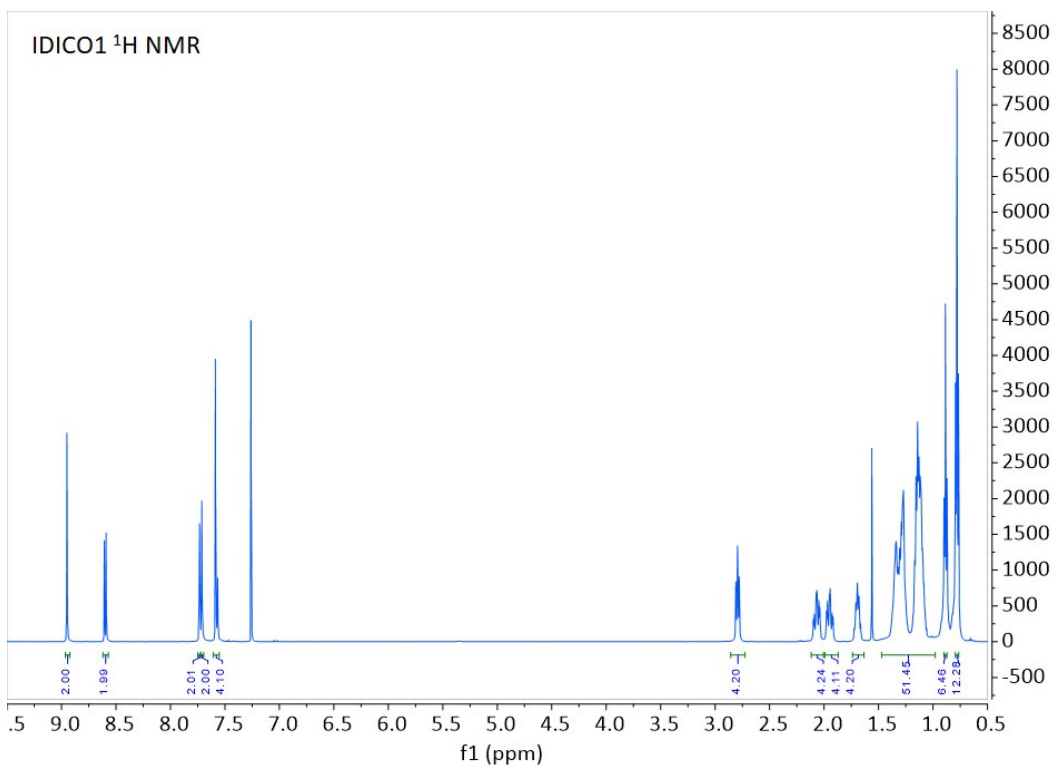


**Figure S12.**  $^1\text{H}$ -NMR spectrum of IDICO1 in  $\text{CDCl}_3$ .

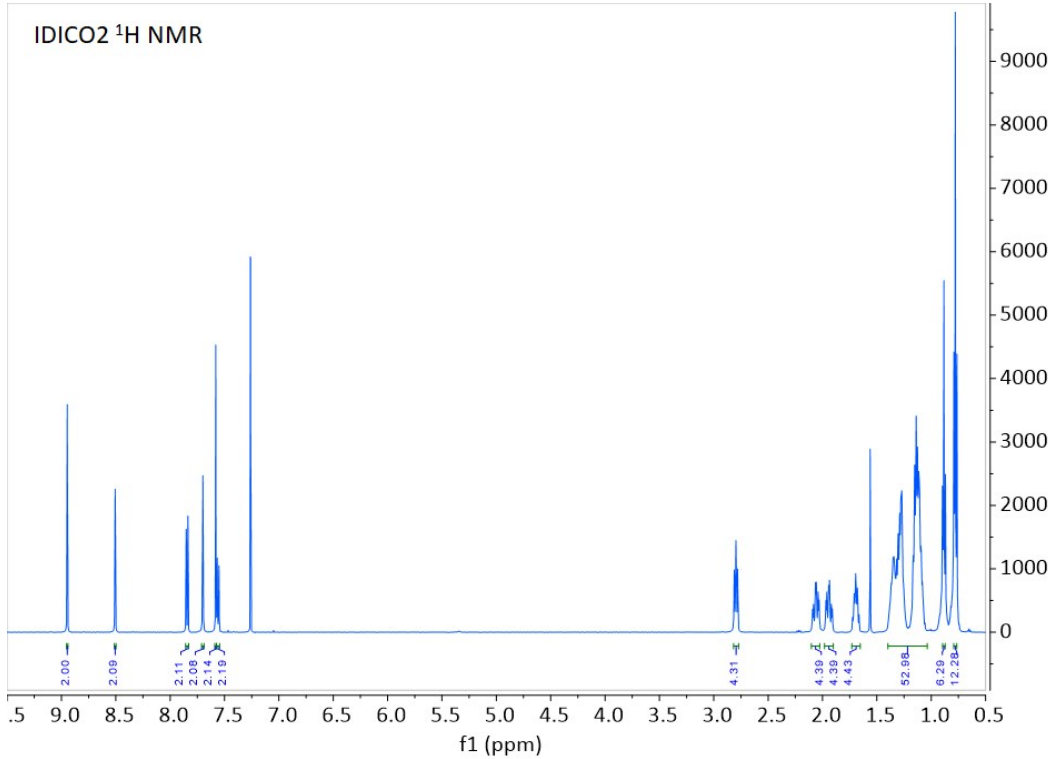


**Figure S13.**  $^1\text{H}$ -NMR spectrum of IDICO2 in  $\text{CDCl}_3$ .

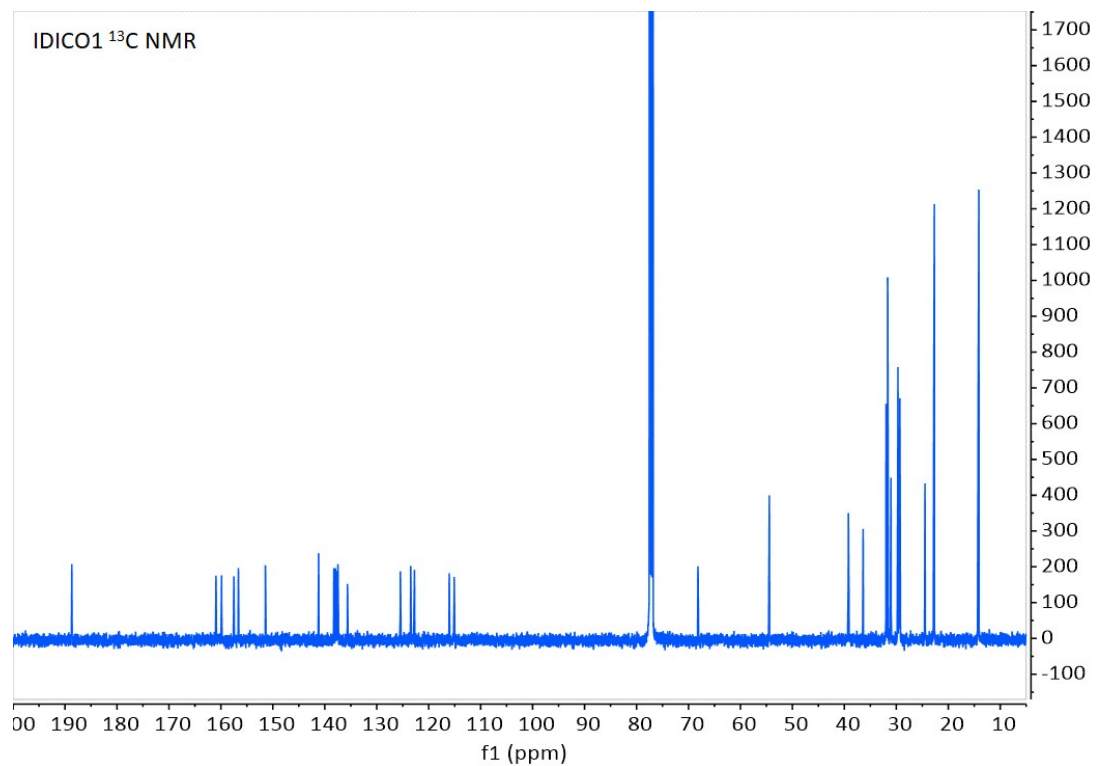


**Figure S14.**  $^{13}\text{C}$ -NMR spectrum of IDICO1 in  $\text{CDCl}_3$ .

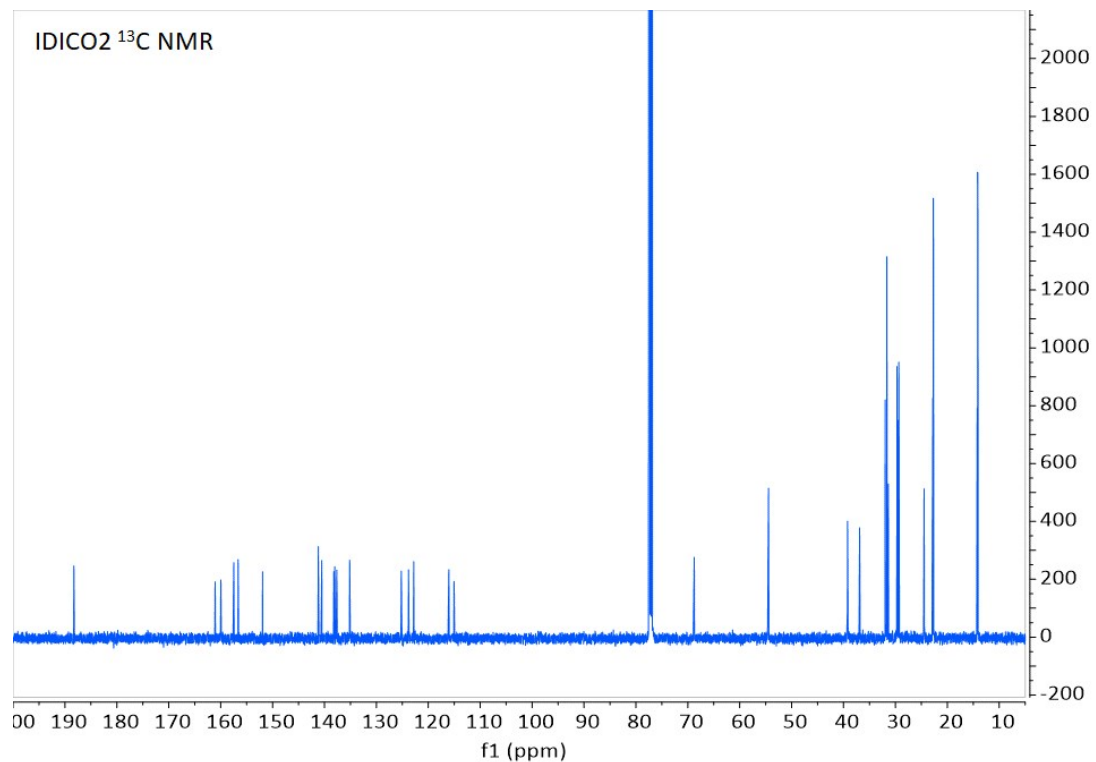


**Figure S15.**  $^{13}\text{C}$ -NMR spectrum of IDICO2 in  $\text{CDCl}_3$ .

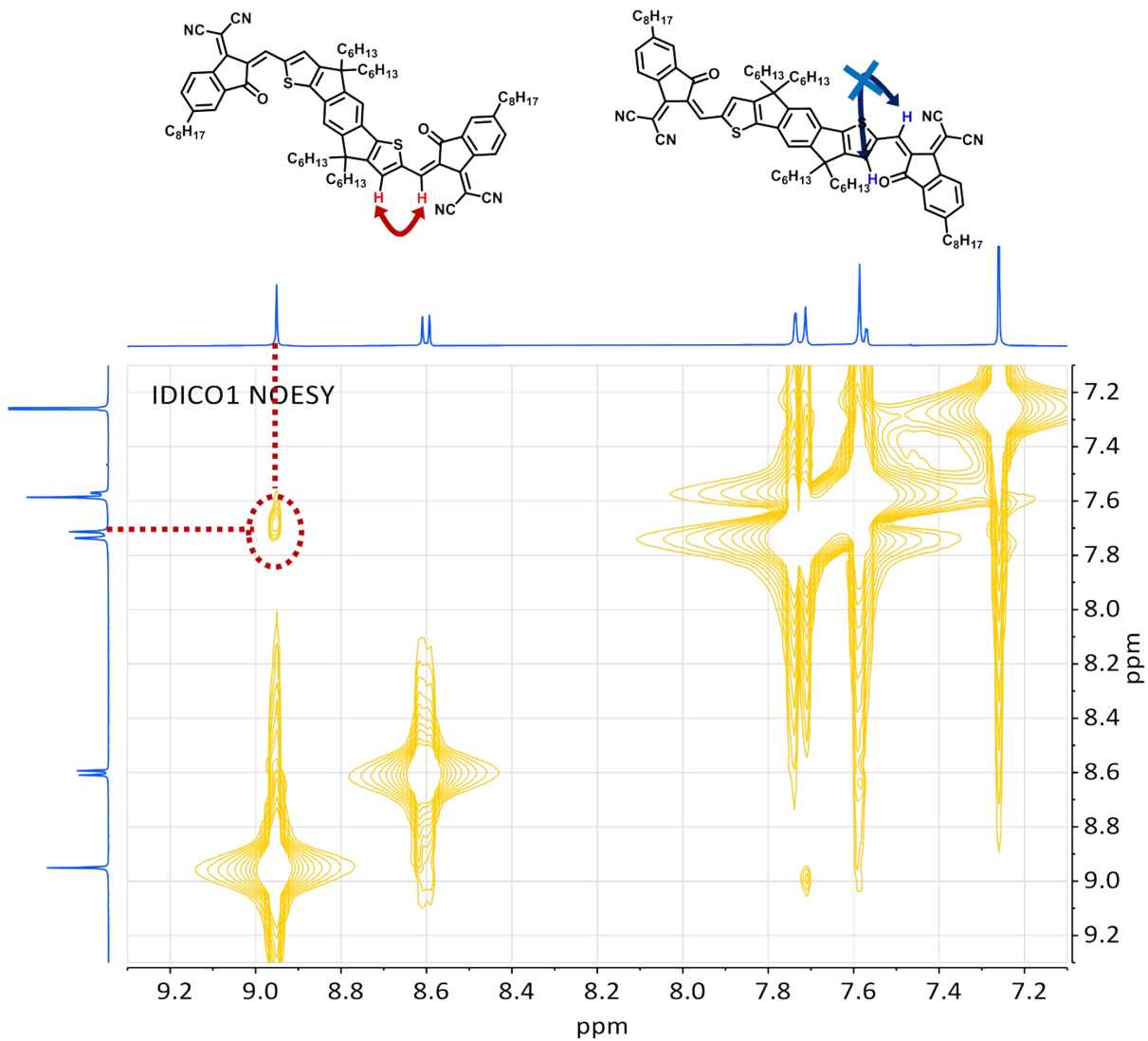


**Figure S16.** 2D NOESY NMR spectrum of IDICO1 in CDCl<sub>3</sub>.

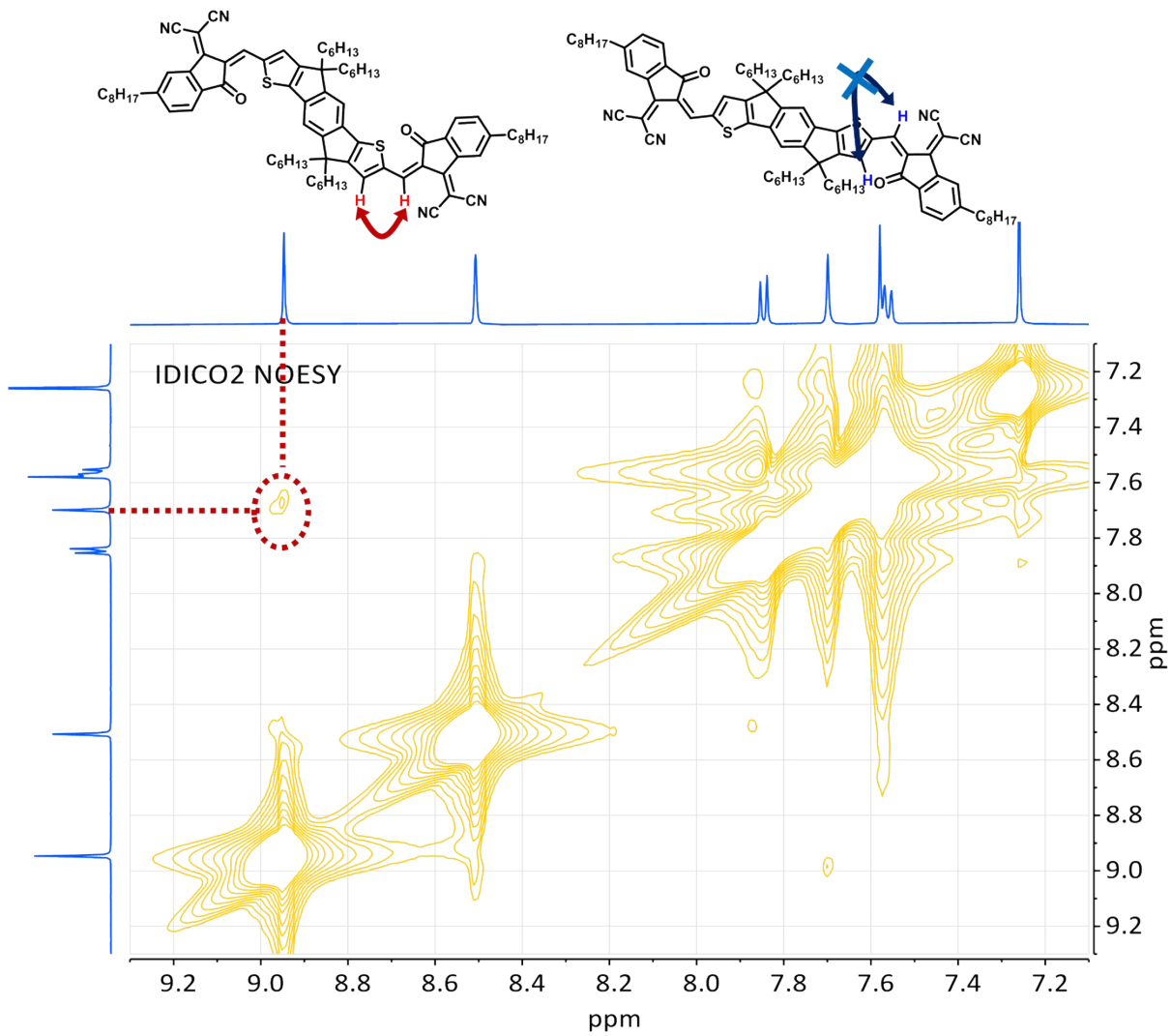


**Figure S17.2D NOESY NMR spectrum of IDICO2 in  $\text{CDCl}_3$ .**

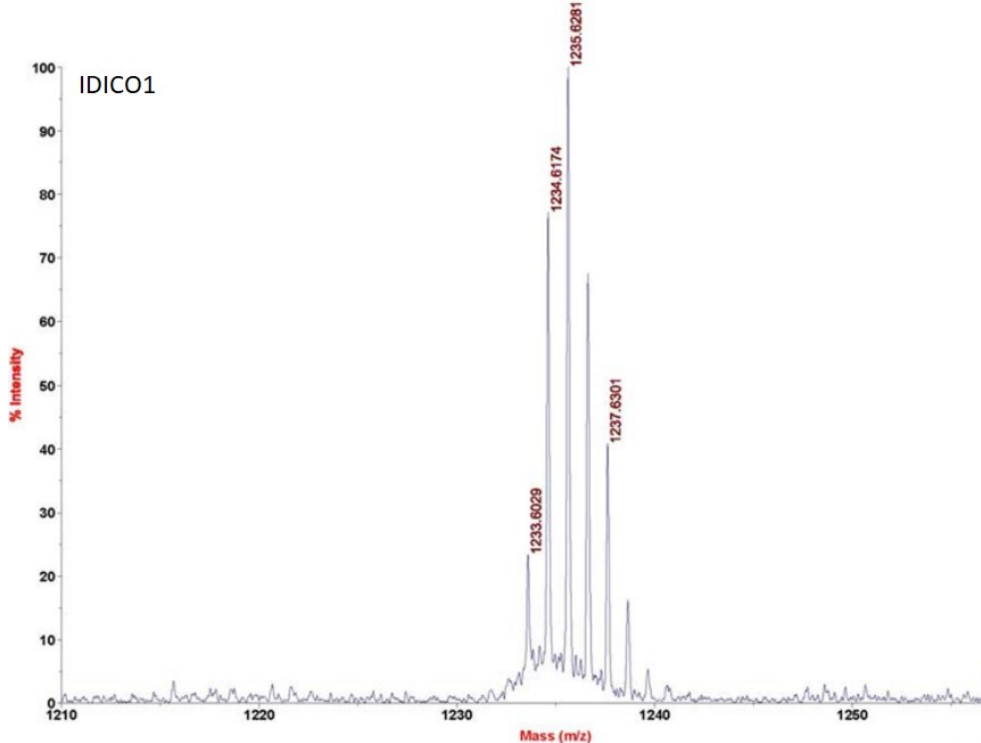


**Figure S18.** MALDI-TOF spectrum of IDICO1.

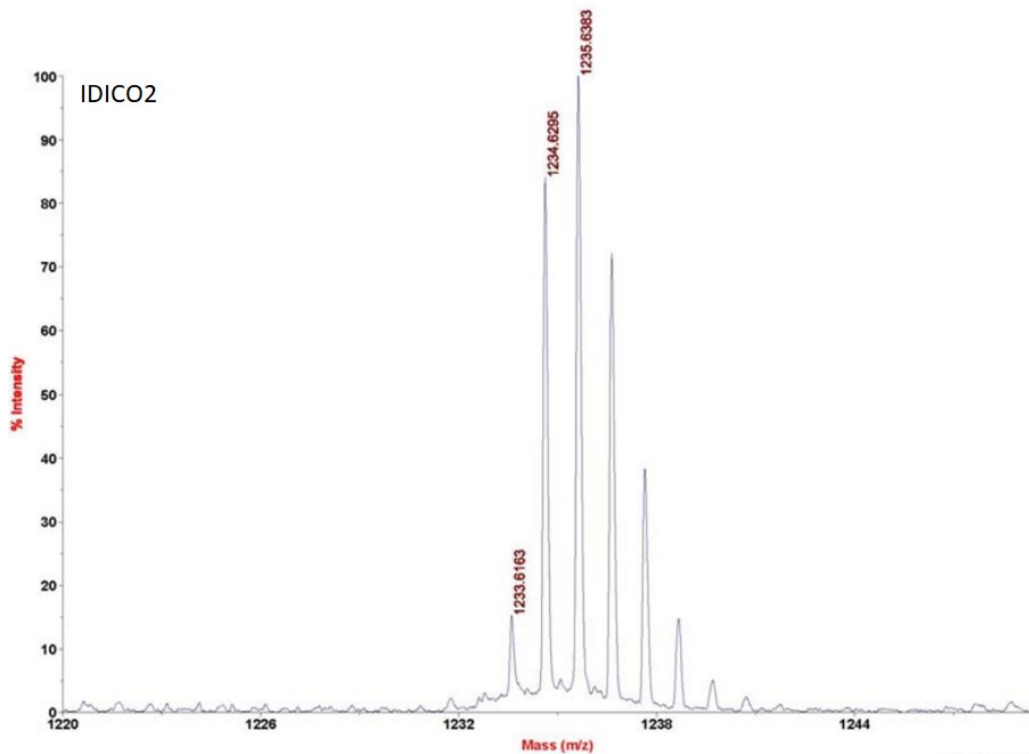


**Figure S19.** MALDI-TOF spectrum of IDICO2.

## Reference

- 1 B. R. Lee, J. S. Goo, Y. W. Kim, Y.-J. You, H. Kim, S.-K. Lee, J. W. Shim and T. G. Kim, *J. Power Sources* **2019**, 417, 61-69.
- 2 Y. J. You, C. E. Song, Q. V. Hoang, Y. Kang, J. S. Goo, D. H. Ko, J. J. Lee, W. S. Shin and J. W. Shim, *Adv. Funct. Mater.* **2019**, 29, 1901171-190118.
- 3 Y. W. Kim, J. S. Goo, T. H. Lee, B. R. Lee, S.-C. Shin, H. Kim, J. W. Shim and T. G. Kim, *J. Power Sources* **2019**, 424, 165-175.
- 4 J. S. Goo, S.-C. Shin, Y.-J. You and J. W. Shim, *Sol. Energy Mater. Sol. Cells* **2018**, 184, 31-37.